

Time-Modulated Phased Array Controlled with Nonideal Bipolar Squared Periodic Sequences

Roberto Maneiro-Catoira, *Member, IEEE*, Julio Brégains, *Senior Member, IEEE*,
José A. García-Naya, *Member, IEEE*, and Luis Castedo, *Senior Member, IEEE*

Abstract—Bipolar (+/-1) sequences with no zero state suit particularly well for safeguarding the switched feeding network efficiency when applied to time-modulated arrays (TMAs). During the zero state of a conventional time-modulating sequence, if a given array element is switched off, a certain amount of energy of the transmitted/received signal is wasted. We propose a novel single sideband time-modulated phased array (TMPA) architecture governed by realistic bipolar squared sequences in which the rise/fall time of the switches is considered. By using single-pole dual-throw switches and non-reconfigurable passive devices, the TMPA exploits, exclusively, the first positive harmonic pattern while exhibiting an excellent performance in terms of efficiency and control level of the undesired harmonics without using synthesis optimization algorithms (software simplicity).

Index Terms—Antenna arrays, time-modulated arrays, beam-steering.

I. INTRODUCTION

PHASED array architectures are based, in general, on variable phase shifters (VPSs). Unfortunately, such devices still exhibit a number of inconveniences such as cost, insertion losses, or phase resolution [1], [2]. The application of switched time-modulated arrays (TMAs) to beam-steering (BS) is attractive in terms of cost and simplicity. However, their efficiency and flexibility must be improved and, particularly, the following concerns are identified in the literature: 1) The lack of efficiency in the distribution of the spectral energy among the working harmonics of rectangular pulses for multiple BS [3]. 2) The overlooking of the presence of mirror-frequency diagrams at the negative harmonics [3]–[5]. 3) The proportionality between the phases of harmonics limits the multiple BS flexibility [6]. 4) The fundamental mode beam has no scanning ability [3], [5], unless supplementary delay lines are included [7]. 5) Defining the overall time-modulation efficiency as $\eta = \eta_{\text{TMA}} \cdot \eta_s$, then $\eta_{\text{TMA}} = P_U^{\text{TM}}/P_R^{\text{TM}}$ (P_U^{TM} and P_R^{TM} are the useful and total mean power values radiated by the TMA, respectively) accounts for the ability of the TMA to filter out and radiate only the useful harmonics and $\eta_s = P_R^{\text{TM}}/P_R^{\text{ST}}$ (P_R^{ST} is the total mean power radiated by

a uniform static array with N elements) accounts for the reduction of the total mean power radiated by a uniform static array caused by the insertion of the TMA switched feeding network. In this respect, the most common is either the switched feeding network efficiency η_s is contemplated but without providing the TMA efficiency η_{TMA} [4], or vice versa [8]. Hence, the efficiency analyses available in the literature are either incomplete or misleading.

Given these shortcomings, in this work we focus our efforts on the design of a switched time-modulated phased array (TMPA) performing BS over a single harmonic.

The main contributions of this work are: 1) The modeling of a single sideband (SSB) switched TMPA architecture governed by bipolar sequences generated by means of single-pole dual-throw (SPDT) switches to efficiently perform BS. 2) The analysis of the impact of the rise/fall time of the SPDT switches on both efficiency factors (η_{TMA} and η_s) and on the control level of the undesired harmonics.

II. DESIGN OF THE SSB TMPA

Any arbitrary periodic waveform (e.g., a square wave) can be expressed, through the trigonometric Fourier series expansion, as an infinite sum (or linear combination) of simple sine and cosine waves. In this letter, however, our aim is to approximate—with a finite sum, see (4) in the forthcoming analysis—a sine wave using a linear combination of non-sinusoidal bipolar square waves¹. In this way, the global idea of this letter is to employ simple time-delayed sine waves (more precisely, good approximations of sine waves) to modulate each antenna array excitation to perform BS. Notice that each sine wave will be synthesized as a linear combination of bipolar square waves which are easily generated by means of SPDT switches.

First, let us study (see Fig. 1) the basic periodic (T_0) bipolar pulse $u(t)$ considered in this work. This pulse models a realistic bipolar ± 1 square periodic pulse, where Δ is the rise/fall time of the switches used to implement such a pulse (hence, from a pure mathematical point of view, they are properly trapezoidal if $\Delta \neq 0$). Its trigonometric Fourier

* Corresponding author: José A. García-Naya (jagarcia@udc.es).

This work has been funded by the Xunta de Galicia (ED431C 2016-045, ED341D R2016/012, ED431G/01), the Agencia Estatal de Investigación of Spain (TEC2015-69648-REDC, TEC2016-75067-C4-1-R) and ERDF funds of the EU (AEI/FEDER, UE).

The authors are with the University of A Coruña, Spain. E-mail: roberto.maneiro@udc.es, julio.bregains@udc.es, jagarcia@udc.es, luis@udc.es

Digital Object Identifier 10.1109/LAWP.2019.2892657

¹We consider non-ideal bipolar waves, which are properly trapezoidal, to model a realistic behavior of the physical switches employed to generate such square waves. The impact of pulse shaping on the sideband radiation of switched TMAs was addressed for the first time in [9] and next in [8].

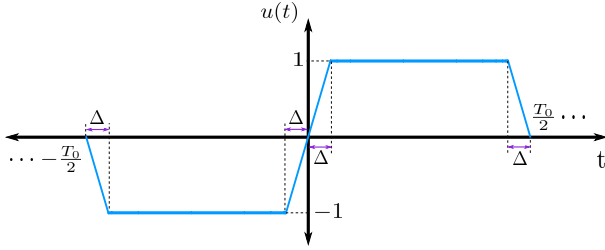


Fig. 1. Periodic bipolar odd pulse. Δ is the rise/fall time of the switches.

coefficients are:

$$U_q = \frac{4}{T_0} \int_0^{T_0/2} u(t) \sin(q\omega_0 t) dt = \begin{cases} \frac{4 \operatorname{sinc}(q\omega_0 \Delta)}{\pi q} & q \text{ odd} \\ 0 & q \text{ even,} \end{cases} \quad (1)$$

with $\omega_0 = 2\pi/T_0$ and, thus, we can write $u(t)$ as

$$u(t) = \frac{4}{\pi} \sum_{q=1,3,5,\dots}^{\infty} \frac{\operatorname{sinc}(q\omega_0 \Delta)}{q} \sin(q\omega_0 t). \quad (2)$$

If we consider a signal $v(t)$ with exactly the same characteristics of $u(t)$ but with triple fundamental frequency, we can express

$$v(t) = \frac{4}{\pi} \sum_{q=1,3,5,\dots}^{\infty} \frac{\operatorname{sinc}(q(3\omega_0)\Delta)}{q} \sin(q(3\omega_0)t), \quad (3)$$

and we can approximate our simple sine function with fundamental frequency ω_0 by means of the linear combination of bipolar periodic signals, i.e.,

$$w(t) = u(t) - 1/3v(t) = \frac{4}{\pi} \sum_{q \in \Upsilon} \frac{\operatorname{sinc}(q\omega_0 \Delta)}{q} \sin(q\omega_0 t), \quad (4)$$

with $\Upsilon = \{q \in \mathbb{N}^*/q \text{ odd}; q \neq \dot{3}\} = \{1, 5, 7, 11, \dots\}$, hence removing the frequencies that are multiple of 3. Additionally, to steer the exploited harmonic pattern of the TMA, we must consider a time-shifted version of $w(t)$, $w_n(t) = w(t - D_n)$, with D_n being the corresponding time-delay variable, hence

$$w_n(t) = \frac{4}{\pi} \sum_{q \in \Upsilon} \frac{\operatorname{sinc}(q\omega_0 \Delta)}{q} \sin(q\omega_0(t - D_n)). \quad (5)$$

Let us now consider a linear TMPA with N isotropic elements with unitary static excitations $I_n = 1$, $n \in \{0, 1, \dots, N-1\}$ whose n -th element feeding scheme is shown in Fig. 2. Such a feeding network has a two-branch structure according to the time-modulating waveform ($w_n(t)$ or $w_n(t - \tau)$)—with τ being a previously fixed time delay—followed by a $\pi/2$ fixed phase shifting. According to Fig. 2, the time-varying array factor is given by

$$F(\theta, t) = \sum_{n=0}^{N-1} \left[\frac{w_n(t)}{\sqrt{2}} + j \frac{w_n(t - \tau)}{\sqrt{2}} \right] e^{jkz_n \cos \theta}, \quad (6)$$

where z_n represents the n -th array element position on the z axis, θ is the angle with respect to such a main axis, and $k = 2\pi/\lambda$ represents the wavenumber for a carrier wavelength $\lambda = 2\pi c/\omega_c$. We begin the analysis of (6) by evaluating the term

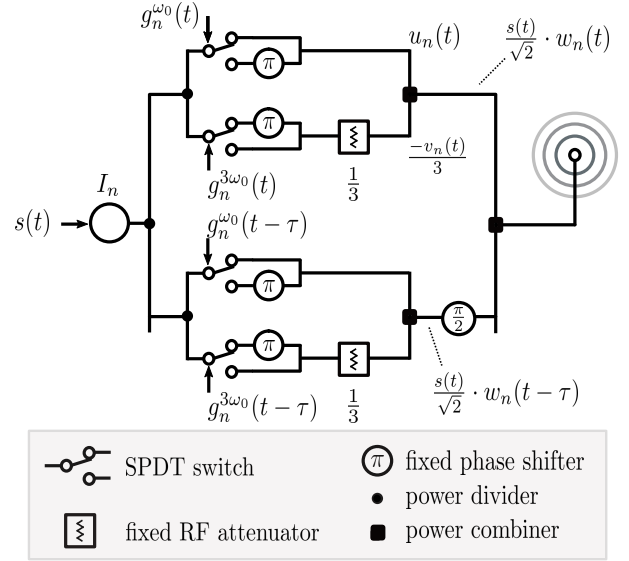


Fig. 2. Scheme of the feeding for the n -th antenna element of the proposed SSB TMPA. Notice that $g_n^{\omega_0}(t)$ and $g_n^{3\omega_0}(t)$ are the corresponding unipolar versions of $u_n(t)$ and $v_n(t)$, which are bipolar.

$w_n(t) + jw_n(t - \tau)$. For the sake of simplicity, we will analyze the Fourier Transform (FT) of such a term, i.e., $\text{FT}[w_n(t)] + j\text{FT}[w_n(t - \tau)]$ where, by virtue of (5),

$$\begin{aligned} \text{FT}[w_n(t)] &= \frac{4}{j} \sum_{q \in \Upsilon} \frac{\operatorname{sinc}(q\omega_0 \Delta)}{q} [e^{-jq\omega_0 D_n} \delta(\omega - q\omega_0) - \\ &\quad - e^{jq\omega_0 D_n} \delta(\omega + q\omega_0)], \text{ and} \\ \text{FT}[w_n(t - \tau)] &= e^{-j\omega\tau} \text{FT}[w_n(t)] = \\ &= \frac{4}{j} \sum_{q \in \Upsilon} \frac{\operatorname{sinc}(q\omega_0 \Delta)}{q} [e^{-jq\omega_0 \tau} e^{-jq\omega_0 D_n} \delta(\omega - q\omega_0) - \\ &\quad - e^{jq\omega_0 \tau} e^{jq\omega_0 D_n} \delta(\omega + q\omega_0)]. \end{aligned} \quad (7)$$

If we select a delay τ verifying that $\omega_0 \tau = \pi/2$, then $e^{-jq\omega_0 \tau} = (-j)^q$ and $e^{jq\omega_0 \tau} = j^q$, and hence we have that

$$\begin{aligned} \text{FT}[w_n(t)] + j\text{FT}[w_n(t - \tau)] &= \\ &= \frac{4}{j} \sum_{q \in \Upsilon} \frac{\operatorname{sinc}(q\omega_0 \Delta)}{q} [(1 - (-j)^{q+1}) e^{-jq\omega_0 D_n} \delta(\omega - q\omega_0) + \\ &\quad + (-1 - j^{q+1}) e^{jq\omega_0 D_n} \delta(\omega + q\omega_0)]. \end{aligned} \quad (8)$$

Considering the sets of indexes $\Upsilon_1 = \{q = 4k - 3; k \in \mathbb{N}^*; q \neq \dot{3}\} = \{1, 5, 13, 17, \dots\}$ and $\Upsilon_2 = \{q = 4k - 1; k \in \mathbb{N}^*; q \neq \dot{3}\} = \{7, 11, 19, 23, \dots\}$, such that $\Upsilon = \Upsilon_1 \cup \Upsilon_2$, then

$$1 - (-j)^{q+1} = \begin{cases} 2 & q \in \Upsilon_1 \\ 0 & q \in \Upsilon_2, \end{cases}; \quad -1 - j^{q+1} = \begin{cases} -2 & q \in \Upsilon_2 \\ 0 & q \in \Upsilon_1. \end{cases} \quad (9)$$

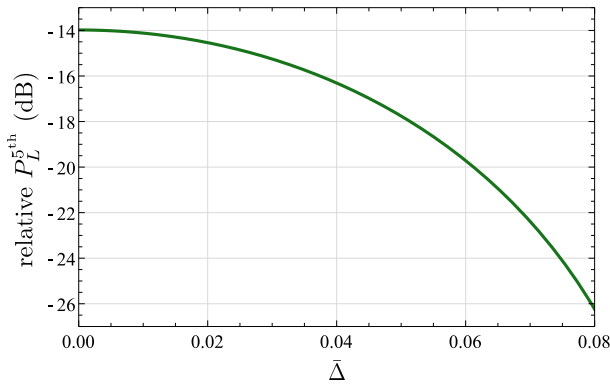


Fig. 3. Representation of the difference between the peak levels of the 1st and 5th harmonics diagrams ($P_L^{5\text{th}}$) as a function of $\bar{\Delta}$ (16). The plot reveals that the peak of the most meaningful undesired harmonic in the proposed TMPA is very sensitive to $\bar{\Delta}$.

Hence, we can rewrite (8) as

$$\begin{aligned} \text{FT}[w_n(t)] + j\text{FT}[w_n(t - \tau)] &= \\ &= \frac{8}{j} \sum_{q \in \Upsilon_1} \frac{\text{sinc}(q\omega_0\Delta)}{q} e^{-jq\omega_0 D_n} \delta(\omega - q\omega_0) + \\ &+ \frac{(-8)}{j} \sum_{q \in \Upsilon_2} \frac{\text{sinc}(q\omega_0\Delta)}{q} e^{jq\omega_0 D_n} \delta(\omega + q\omega_0), \end{aligned} \quad (10)$$

and we realize that the harmonics with orders $-1, -5, 7, 11, \dots$ are removed. By applying the inverse FT to (10), we have

$$\begin{aligned} w_n(t) + jw_n(t - \tau) &= \sum_{q \in \Upsilon_1} \frac{4 \text{sinc}(q\omega_0\Delta)}{j\pi q} e^{-jq\omega_0 D_n} e^{jq\omega_0 t} + \\ &+ \sum_{q \in \Upsilon_2} \frac{-4 \text{sinc}(q\omega_0\Delta)}{j\pi q} e^{jq\omega_0 D_n} e^{-jq\omega_0 t}, \end{aligned} \quad (11)$$

and (6) can be rewritten as

$$\begin{aligned} F(\theta, t) &= \frac{1}{\sqrt{2}} \sum_{n=0}^{N-1} \left[\sum_{q \in \Upsilon_1} \frac{4 \text{sinc}(q\omega_0\Delta)}{j\pi q} e^{-jq\omega_0 D_n} e^{jq\omega_0 t} + \right. \\ &\left. + \sum_{q \in \Upsilon_2} \frac{-4 \text{sinc}(q\omega_0\Delta)}{j\pi q} e^{jq\omega_0 D_n} e^{-jq\omega_0 t} \right] e^{jkz_n \cos \theta}. \end{aligned} \quad (12)$$

We now define

$$\begin{aligned} F_1(\theta, t)_q &= e^{jq\omega_0 t} \sum_{n=0}^{N-1} I_{nq} e^{jkz_n \cos \theta}, \quad \text{and} \\ F_2(\theta, t)_q &= e^{-jq\omega_0 t} \sum_{n=0}^{N-1} I'_{nq} e^{jkz_n \cos \theta}, \end{aligned} \quad (13)$$

to finally obtain

$$F(\theta, t) = \sum_{q \in \Upsilon_1} F_1(\theta, t)_q + \sum_{q \in \Upsilon_2} F_2(\theta, t)_q, \quad (14)$$

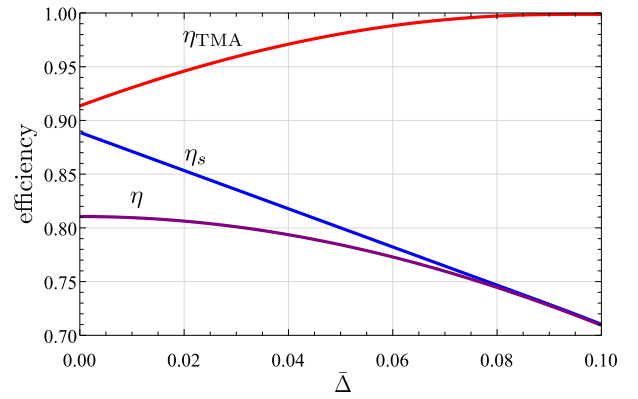


Fig. 4. Efficiencies of the TMPA as a function of the normalized rise/fall time of the SPDT switches $\bar{\Delta}$.

where the dynamic excitations I_{nq} and I'_{nq} are given by

$$\begin{aligned} I_{nq} &= \frac{4 \text{sinc}(q\omega_0\Delta)}{j\pi\sqrt{2}q} e^{-jq\omega_0 D_n}, \quad q \in \Upsilon_1, \quad \text{and} \\ I'_{nq} &= \frac{-4 \text{sinc}(q\omega_0\Delta)}{j\pi\sqrt{2}q} e^{jq\omega_0 D_n}, \quad q \in \Upsilon_2, \end{aligned} \quad (15)$$

III. IMPACT OF Δ ON THE TMPA PERFORMANCE

In this section, we analyze 1) the effects produced by Δ on the peak level of the power radiated pattern at the most meaningful undesired harmonic (i.e., $|F_1(\theta, t)_5|^2$) with respect to the peak level at the exploited harmonic ($|F_1(\theta, t)_1|^2$); and 2) the impact of Δ on the efficiency of the time modulation operation applied to the TMPA. Regarding the first aim, according to (15), and by considering the normalized rise/fall time of the switches $\bar{\Delta} = \Delta/T_0$, we define the figure of merit

$$P_L^{5\text{th}} \text{ (dB)} = 20 \log_{10} \left| \frac{I_{n5}}{I_{n1}} \right| = 20 \log_{10} \left| \frac{\text{sinc}(10\pi\bar{\Delta})}{5 \text{sinc}(2\pi\bar{\Delta})} \right|, \quad (16)$$

which quantifies the difference, in dB, between the peak levels of the 1st and 5th harmonics diagrams. The representation of $P_L^{5\text{th}}$ as a function of $\bar{\Delta}$ —according to (16)—is shown in Fig. 3, which illustrates that it is possible to keep $P_L^{5\text{th}}$ below a predetermined threshold by selecting an appropriate value of $\bar{\Delta}$. Hence, $\bar{\Delta}$ manifests itself as a crucial design parameter.

However, $\bar{\Delta}$ also impacts on the efficiency of the time modulation operation in the TMPA. As described in the introduction, such an efficiency depends on two factors: η_{TMA} and η_s . Hence, the selection of $\bar{\Delta}$ impacts not only on η_{TMA} (as described in [8] using other kind of pulses and hardware), but also (and this constitutes a key contribution of this work) on η_s and, consequently, on the overall efficiency η .

We next accurately characterize the variation of both terms of η with Δ . To simplify the analysis, but without any relevant loss of generality, we consider a uniform linear array with inter-element distance of $\lambda/2$ transmitting a single carrier with normalized power. We start by quantifying P_R^{TM} , the total mean radiated power by the TMPA, which is given by the expression $P_R^{\text{TM}} = \sum_{q \in \Upsilon_1} (p_1)_q + \sum_{q \in \Upsilon_2} (p_2)_q$, see [3, (16)], being $(p_1)_q$ and $(p_2)_q$ the total mean radiated power values at the frequencies $\omega_c + q\omega_0$ with $q \in \Upsilon_1$ and $\omega_c - q\omega_0$ with $q \in \Upsilon_2$, respectively. As $(p_1)_q =$

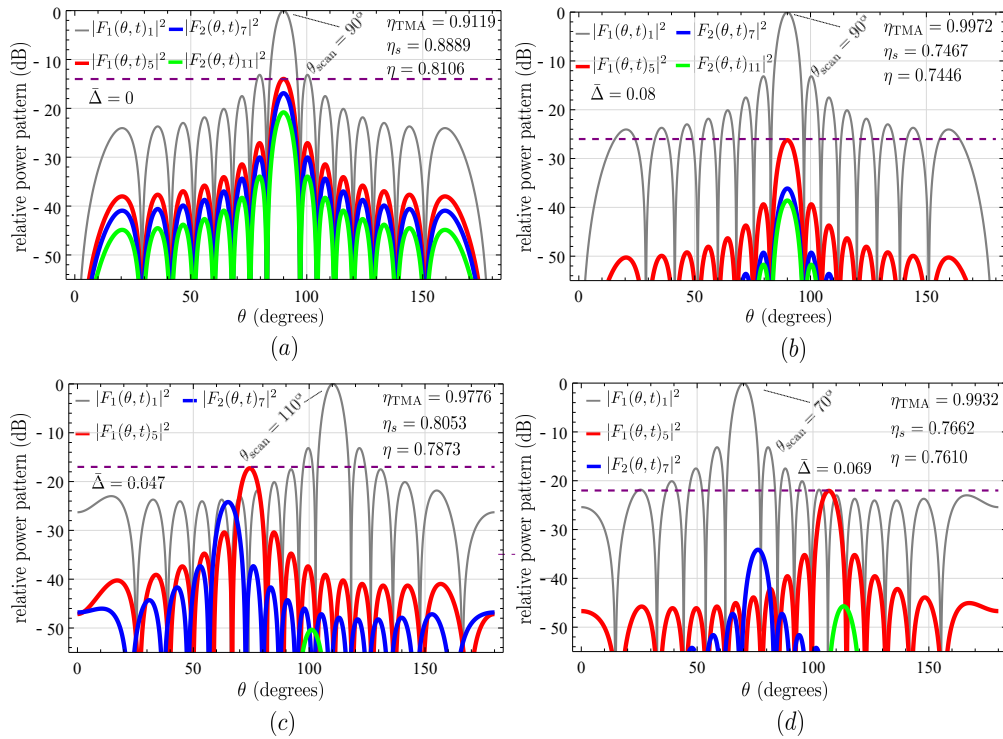


Fig. 5. Relative power radiated patterns of the proposed TMPA with $N = 16$ for different normalized rise/fall time of the SPDT switches $\bar{\Delta}$ and time delays D_n . The scenarios (a) to (d) are explained in Section IV.

$4\pi \sum_{n=0}^{N-1} |I_{nq}|^2$ and $(p_2)_q = 4\pi \sum_{n=0}^{N-1} |I'_{nq}|^2$, see [3], and $|I_{nq}|^2 = |I'_{nq}|^2 = 8 \text{sinc}^2(q\omega_0\bar{\Delta})/(\pi^2 q^2)$ from (15), we arrive at $P_R^{\text{TM}} = \frac{32N}{\pi} \sum_{q \in \Upsilon} \frac{\text{sinc}^2(q\omega_0\bar{\Delta})}{q^2}$. Notice that the useful mean radiated power is $P_U^{\text{TM}} = (p_1)_1 = 4\pi \sum_{n=0}^{N-1} |I_{n1}|^2 = 32N \text{sinc}^2(\omega_0\bar{\Delta})/\pi$. On the other hand, the total mean power radiated by a uniform static array with N elements, P_R^{ST} , is calculated as the total mean transmitted power over the array factor $F^{\text{ST}}(\theta) = \sum_{n=0}^{N-1} e^{jkz_n \cos \theta}$ and, hence, $P_R^{\text{ST}} = \int_0^{2\pi} \int_0^\pi |F^{\text{ST}}(\theta)|^2 \sin(\theta) d\theta d\varphi = 4\pi N$. Therefore:

$$\eta_{\text{TMA}}(\bar{\Delta}) = \frac{P_U^{\text{TM}}}{P_R^{\text{TM}}} = \frac{\text{sinc}^2(2\pi\bar{\Delta})}{\sum_{q \in \Upsilon} \frac{\text{sinc}^2(2\pi q\bar{\Delta})}{q^2}}, \text{ and} \quad (17)$$

$$\eta_s(\bar{\Delta}) = \frac{P_R^{\text{TM}}}{P_R^{\text{ST}}} = \frac{8}{\pi^2} \sum_{q \in \Upsilon} \frac{\text{sinc}^2(2\pi q\bar{\Delta})}{q^2}, \quad (18)$$

and consequently,

$$\eta(\bar{\Delta}) = \eta_{\text{TMA}}(\bar{\Delta}) \cdot \eta_s(\bar{\Delta}) = \frac{8}{\pi^2} \text{sinc}^2(2\pi\bar{\Delta}). \quad (19)$$

Fig. 4 illustrates the different TMPA efficiencies as a function of $\bar{\Delta}$. From Figs. 3 and 4 we observe that the better the $P_L^{5\text{th}}$, the better the η_{TMA} , as expected. We also appreciate the opposite slopes of both factors of the efficiency. Finally, we highlight the existence of a trade-off between $P_L^{5\text{th}}$ and η when $\bar{\Delta}$ changes. Such a factor should be accurately taken into account by the antenna designer.

IV. NUMERICAL SIMULATIONS

In this section, we show the behavior of the proposed TMPA by means of several numerical examples. In line with Figs. 3

and 4, Fig. 5a shows that when $\bar{\Delta} = 0$ (ideal squared pulses), $P_L^{5\text{th}}$ (-14 dB) and η_{TMA} (91%) exhibit their worst values while η_s (89%) and η (81%) achieve their best values, and the directivity $G_D = 11.64$ dBi. Notice that the time-delays D_n are set to zero, and hence the scanning angle of all patterns (see (12)) will be $\theta_{\text{scan}} = 90^\circ$.

In Fig. 5b, without varying θ_{scan} , $\bar{\Delta}$ is raised to 0.08 and we observe that $G_D = 12.03$ dBi and both $P_L^{5\text{th}}$ (-26 dB) and η_{TMA} are sensibly improved (87.7% and 9.35%, respectively) at the expense of a worse η_s (decreased to 16.0%), and leading also to a worse η (a reduction of 8.14%).

Figs. 5c and 5d show both the scanning ability of the TMPA and the trade off between η and $P_L^{5\text{th}}$ when different values of $\bar{\Delta}$ are selected. More specifically, the $P_L^{5\text{th}}$ threshold in Fig. 5c is fixed at -17 dB and, according to (16) and Fig. 3, $\bar{\Delta} = 0.047$, thus achieving an η that is only 2.9% below its maximum value while $G_D = 11.94$ dBi. In this case, D_n are selected to accomplish a $\theta_{\text{scan}} = 110^\circ$ by simply assigning progressive phases to the array elements, i.e., considering $D_n/T_0 = n \cos(\theta_{\text{scan}})$. In Fig. 5d, the $P_L^{5\text{th}}$ threshold is fixed at a more stringent level, -22 dB, which leads to $\bar{\Delta} = 0.069$, thus achieving an η which is 6.1% below its maximum value. In this case, D_n are selected to accomplish a $\theta_{\text{scan}} = 70^\circ$ while $G_D = 12.01$ dBi. Notice that, since all the excitations of the patterns are uniform, the sideband-lobe level (SLL) and the half-power beam-width (HPBW) only depend on N .

V. CONCLUSIONS

We proposed a novel TMPA scheme based on time modulation with non-ideal bipolar squared periodic sequences. When

the rise/fall time of the pulses changes, we have accurately analyzed the trade off between the two components of the time modulation efficiency, as well as the trade off between such an efficiency and the peak level of the most meaningful undesired harmonic. Accordingly, the structure presents the advantage that the designer can select an adequate rise/fall time of the bipolar pulses (and therefore, a particular SPDT switch) in order to guarantee a certain threshold for the undesired harmonics while the efficiency of the time modulation remains above the value dictated by the required performance level.

REFERENCES

- [1] "Qorvo," <http://www.qorvo.com>, monolithic microwave integrated circuit (MMIC) digital phase shifters. Accessed: 2018-08-08.
- [2] J. P. González-Coma, R. Maneiro-Catoira, and L. Castedo, "Hybrid precoding with time-modulated arrays for mmwave mimo systems," *IEEE Access*, vol. 6, pp. 59 422–59 437, 2018.
- [3] R. Maneiro Catoira, J. Brégains, J. A. Garcia-Naya, L. Castedo, P. Rocca, and L. Poli, "Performance analysis of time-modulated arrays for the angle diversity reception of digital linear modulated signals," *IEEE J. Sel. Topics Signal Process.*, vol. 11, no. 2, pp. 247–258, Mar. 2017.
- [4] G. Bogdan, Y. Yashchynshyn, and M. Jarzynka, "Time-modulated antenna array with lossless switching network," *IEEE Antennas Wireless Propag. Lett.*, vol. 15, pp. 1827–1830, Mar. 2016.
- [5] L. Poli, P. Rocca, G. Oliveri, and A. Massa, "Harmonic beamforming in time-modulated linear arrays," *IEEE Trans. Antennas Propag.*, vol. 59, no. 7, pp. 2538–2545, Jul. 2011.
- [6] R. Maneiro Catoira, J. Brégains, J. A. Garcia-Naya, and L. Castedo, "Enhanced time-modulated arrays for harmonic beamforming," *IEEE J. Sel. Topics Signal Process.*, vol. 11, no. 2, pp. 259–270, Mar. 2017.
- [7] C. Sun, S. Yang, Y. Chen, J. Guo, and Z. Nie, "An improved phase modulation technique based on four-dimensional arrays," *IEEE Antennas Wireless Propag. Lett.*, vol. 16, pp. 1175–1178, Nov. 2016.
- [8] A. M. Yao, W. Wu, and D. G. Fang, "Single-sideband time-modulated phased array," *IEEE Trans. Antennas Propag.*, vol. 63, no. 5, pp. 1957–1968, May 2015.
- [9] E. T. Bekele, L. Poli, P. Rocca, M. D'Urso, and A. Massa, "Pulse-shaping strategy for time modulated arrays—analysis and design," *IEEE Trans. Antennas Propag.*, vol. 61, no. 7, pp. 3525–3537, Jul. 2013.